

Tuning of Electronic Structures of Quasi-One-Dimensional Bromo-Bridged Pd^{II}–Pd^{IV} Mixed-Valence Complexes by Substituting Counter Anions

Hisamitsu Arakawa,¹ Daisuke Kawakami,²
Shinya Takaishi,² Takashi Kajiwara,²
Hitoshi Miyasaka,¹ Ken-ichi Sugiura,¹
Masahiro Yamashita,^{*2} Hideo Kishida,³
and Hiroshi Okamoto³

¹Department of Chemistry, Graduate School of Science,
Tokyo Metropolitan University, Minamioshima,
Hachioji, Tokyo 192-0397

²Department of Chemistry, Graduate School of Science,
Tohoku University & CREST(JST), Aoba-ku,
Sendai 980-8578

³Department of Advanced Materials Science, Graduate
School of Frontier Science, The University of Tokyo,
515 Kashiwanoha, Kashiwa 277-8561

Received February 15, 2006; E-mail: yamasita@agnus.chem.
tohoku.ac.jp

New quasi-one-dimensional bromo-bridged Pd^{II}–Pd^{IV} mixed-valence complexes with long chain alkylsulfonates [Pd(en)₂][PdBr₂(en)](C_nH_{2n+1}SO₃)₄·2H₂O (en = ethylenediamine, *n* = 7, 8, 9, and 10) were synthesized. With increasing alkyl-chain length (*n*) of the counter anions, the Pd^{II}...Pd^{IV} distances decreased, indicating that the oxidation states of the Pd atoms are close to the Pd^{III} state.

Quasi-one-dimensional halogen-bridged mixed-valence complexes (MX chains) have been attracting much attention because they show very interesting physical properties, such as intense and dichroic inter-valence charge-transfer bands, progression in the resonance Raman spectra, luminescence spectra with large Stokes-shifts, large third-order nonlinear optical properties, midgap absorptions attributable to solitons, polarons, etc.¹ Theoretically, these MX chains are considered to be extended Peierls–Hubbard systems, where electron-phonon interaction (*S*), electron transfer (*T*), on- and neighbor-site Coulomb repulsion energies (*U* and *V*, respectively) compete or cooperate with each other.²

The Pt and Pd complexes take charge density wave (CDW) or M^{II}–M^{IV} mixed-valence states due to *S*, where the bridging halides are displaced from the midpoints between the neighboring two metal ions (Fig. 1a). Therefore, these Pt and Pd complexes are class II type for mixed-valence compounds in the Robin and Day classification.³ In these MX chain com-

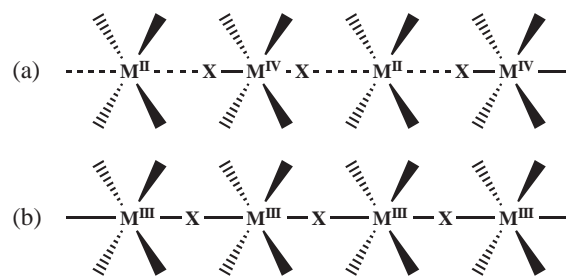


Fig. 1. Structure of M^{II}–M^{IV} mixed-valence complexes of Pt and Pd (a), and M^{III} complexes of Ni (b).

plexes, the CDW amplitudes can be tuned by varying metal ions, bridging halide ions, in-plane ligands, and counter anions.⁴ Moreover, the dimensionalities of the CDW can be controlled by using the intra- and inter-chain hydrogen-bond networks.⁵

On the other hand, Ni complexes take Ni^{III} Mott–Hubbard states due to the strong *U*, where the bridging halides are located at the midpoints between neighboring two Ni atoms (Fig. 1b). Very strong antiferromagnetic interactions among spins located on the Ni^{III} d_{z²} orbitals through the bridging halide ions are observed in these complexes.⁶ Therefore, the Ni complexes are class III type for mixed-valence compounds in the Robin and Day classification. These complexes have also been of recent interest in applied science because a gigantic third-order nonlinear optical susceptibility ($\approx 10^{-4}$ e.s.u.) has been observed for [Ni^{III}(chxn)₂Br]Br₂ (chxn = 1*R*,2*R*-diaminocyclohexane).⁷

More recently, a new series of MX chains, that is, the Ni–Pd mixed-metal complexes Ni_{1–*x*}Pd_{*x*}(chxn)₂Br₃, have been synthesized, where *S* on the Pd sites and *U* on the Ni sites compete with each other. With an increase in the Ni component, the Pd^{II}–Pd^{IV} mixed-valence state gradually changed to the Pd^{III} state due to the stronger *U* on the Ni site (≈ 5 eV) compared with *S* on the Pd site (≈ 1 eV).⁸ Their local electronic structures, such as Mott–Hubbard state, CDW state, and soliton, have been directly observed by scanning tunneling microscopy (STM) for the first time.⁹

The number of Pd^{II}–Pd^{IV} mixed-valence complexes is less than that of Pt^{II}–Pt^{IV} mixed-valence complexes, because the Pd^{IV} states are less stable compared with the Pt^{IV} states. Therefore, the counter ions of Pd^{II}–Pd^{IV} complexes with ethylenediamine (en) ligand occur only with ClO₄[–] and BF₄[–],¹⁰ affording relatively weak *T*. In order to promote interaction between the Pd^{II} site and the Pd^{IV} site, or to generate the Pd^{III} Mott–Hubbard state, we have synthesized new Pd^{II}–Pd^{IV} mixed-valence complexes with en as an in-plane ligand by substituting the counter anions with C_nH_{2n+1}SO₃[–] (*n* = 7, 8, 9, and 10), which are expected to form different hydrogen-bonds between NH₂ of en and O of C_nH_{2n+1}SO₃[–], as well as cause fastener effects. Similar Pt^{II}–Pt^{IV} mixed-valence complexes have been studied by Matsushita and Taira.¹¹ However, no Pd complexes with C_nH_{2n+1}SO₃[–] counter anions have been reported.

Single-crystal X-ray structure determination was carried out for all complexes at 93 K. Figure 2 shows two perspective views of the *n* = 7 complex. The planar [Pd(en)₂] units are

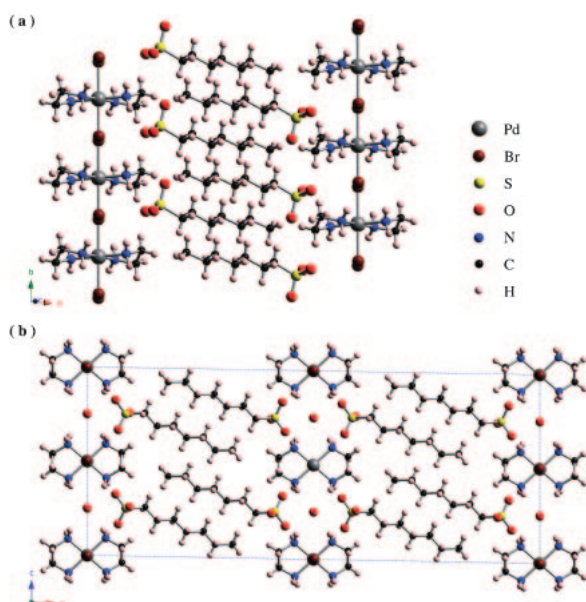


Fig. 2. Perspective views of the 3D packing of $[\text{Pd}(\text{en})_2][\text{PdBr}_2(\text{en})_2](\text{C}_7\text{H}_{15}\text{SO}_3)_4$.

Table 1. Comparison of the Interatomic Distances along the Chains (\AA)

n	$\text{Pd}^{\text{II}}\text{--Pd}^{\text{IV}}$	$\text{Pd}^{\text{IV}}\text{--X}$	$\text{X}\cdots\text{Pd}^{\text{II}}$	d^{a}
7	5.283(4)	2.498(4)	2.785(4)	0.054
8	5.3018(9)	2.499(3)	2.803(3)	0.057
9	5.274(3)	2.496(4)	2.778(4)	0.053
10	5.292(4)	2.489(4)	2.803(4)	0.059
ClO_4	5.407	2.496	2.911	0.077

a) $d = \{(\text{X}\cdots\text{Pd}^{\text{II}}) - (\text{Pd}^{\text{IV}}\text{--X})\}/(\text{Pd}^{\text{II}}\cdots\text{Pd}^{\text{IV}})$.

bridged by Br ions, which are disordered at positions away from the midpoints between two neighboring Pd ions with half occupancies, thus forming linear chain $\text{Pd}^{\text{II}}\text{--Pd}^{\text{IV}}$ mixed-valence structures. In order to understand the inter-chain valence arrangement, X-ray diffuse scattering was measured for these complexes. As a result, a rod-shaped diffuse scattering was observed in all complexes, indicating that these complexes are in a two-dimensional CDW state, where the CDW phase is ordered in the bc -plane.⁵ As a comparison with the complex of ClO_4^- , the relevant bond distances are listed in Table 1. The $\text{Pd}\cdots\text{Pd}$ distance, $\text{Pd}^{\text{IV}}\text{--Br}$ and $\text{Pd}^{\text{II}}\cdots\text{Br}$ bond lengths of the $n = 7$ complex are 5.283, 2.499, and 2.784 \AA , respectively, while those in $[\text{Pd}(\text{en})_2][\text{PdBr}_2(\text{en})_2](\text{ClO}_4)_4$ are 5.407, 2.496, and 2.911 \AA , respectively.¹² The degrees of displacements of the bridging halide ions from the midpoints between two neighboring Pd ions, defined as $\{(\text{X}\cdots\text{Pd}^{\text{II}}) - (\text{Pd}^{\text{IV}}\text{--X})\}/(\text{Pd}^{\text{II}}\cdots\text{Pd}^{\text{IV}})$, are 0.054 for the former complex and 0.077 for the latter. Therefore, the oxidation state of the present complex is closer to Pd^{III} , namely a Robin–Day class III complex, than the complex with ClO_4^- .

Single-crystal reflectance spectra of $[\text{Pd}(\text{en})_2][\text{PdBr}_2(\text{en})_2](\text{C}_n\text{H}_{2n+1}\text{SO}_3)_4$ ($n = 7, 8, 9$, and 10) were measured at room temperature. Optical conductivities obtained from the Kramers–Kronig transformation are shown in Fig. 3. The $n =$

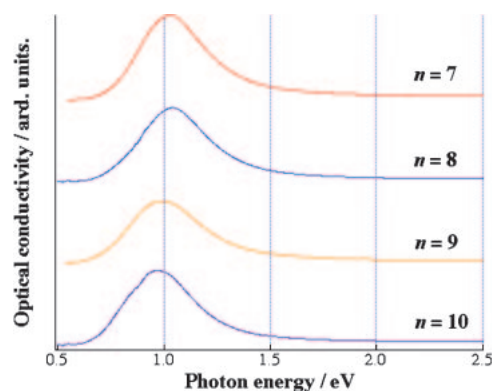


Fig. 3. Optical conductivity spectra with polarization of light parallel to the b axis in $[\text{Pd}(\text{en})_2][\text{PdBr}_2(\text{en})_2](\text{C}_n\text{H}_{2n+1}\text{SO}_3)_4$ ($n = 7, 8, 9$, and 10).

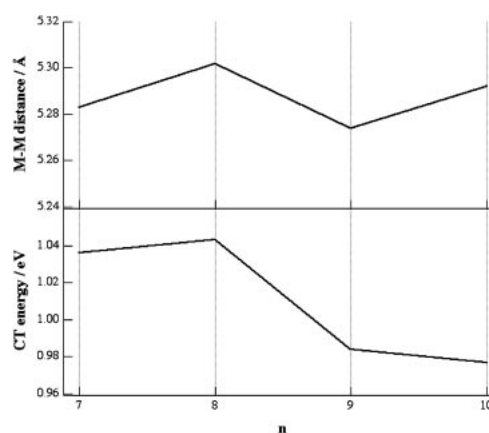


Fig. 4. The parity behavior of the M–M distance and the CT energy of $[\text{Pd}(\text{en})_2][\text{PdBr}_2(\text{en})_2](\text{C}_n\text{H}_{2n+1}\text{SO}_3)_4$ ($n = 7, 8, 9$, and 10).

7 complex showed an intense band at 1.03 eV. This is attributed to a charge-transfer (CT) transition from the Pd^{II} species to the Pd^{IV} species along the chain. According to theoretical studies,¹³ the energy of the CT bands in mixed-valence compounds is given a $2S - U$, if T and V are neglected. The lower CT energy of the present complex than the complex of ClO_4^- (1.13 eV¹⁴) is a consequence of a decrease in S , suggesting that the charge delocalization of this complex is larger than that of the complex of ClO_4^- . This is consistent with the finding that the displacement of the bridging bromide ions in the present complexes is smaller than that of the complexes of ClO_4^- as discussed above. This can be explained by the difference in the hydrogen-bond modes, i.e., $\text{HN}\cdots\text{O}\cdots\text{HN}$ (via one atom) in the present complexes, while $\text{NH}\cdots\text{O}\cdots\text{Cl}\cdots\text{O}\cdots\text{HN}$ (via three atoms) in complex of ClO_4^- .

Moreover, the $\text{Pd}\cdots\text{Pd}$ distance and the CT energy decreased with increasing alkyl-chain length with parity behavior as shown in Fig. 4. The unit cell angle β also shows this parity behavior depending on the alkyl-chain length, i.e., $\beta = 91.033(9), 97.060(11), 93.456(7)$, and $99.086(9)^\circ$ for $n = 7, 8, 9$, and 10 , respectively. This is presumably due to the difference in the crystal packing arising from the difference in the alkyl-chain length.

In this work, the new quasi-one-dimensional bromo-bridged Pd^{II}–Pd^{IV} mixed-valence complexes with long chain alkylsulfonates counter anion were synthesized. These complexes have a different hydrogen-bond mode from that of complexes with ClO₄[−]. The results of X-ray and optical conductivity measurements indicates that the oxidation states of Pd atoms approach the Pd^{III} state with increasing alkyl-chain length, which is presumably due to the fastener effects of the long alkyl-chains of the counter anions.

Experimental

Syntheses. The starting material, [Pd(en)₂]Br₂ was synthesized by mixing PdBr₂ (3 g, 11.3 mmol) and ethylenediamine (4.5 g, 74.8 mmol) in aqueous solution: 4.06 g (10.5 mmol, 93.2%). The compound [Pd(en)₂][PdBr₂(en)](C_nH_{2n+1}SO₃)₄·2H₂O (*n* = 7, 8, 9, and 10) were obtained by diffusing Br₂ gas to the 5 mL aqueous solution containing C_nH_{2n+1}SO₃Na (*n* = 7, 8, 9, and 10) (300 mg, excess) and [Pd(en)₂]Br₂ (100 mg, 0.259 mmol).

Single crystal X-ray structure was determined using RIGAKU MSC SATURN CCD diffractometer with graphite monochromator Mo Kα (λ = 0.7107 Å). Crystal data for [Pd(en)₂][PdBr₂(en)](C₇H₁₅SO₃)₄·2H₂O at 93(2) K: *M*_r = 683.03, monoclinic, space group C2/c, *a* = 36.48(3) Å, *b* = 5.283(4) Å, *c* = 15.237(11) Å, β = 91.033(9)°, *V* = 2936(4) Å³, *Z* = 4, ρ_{calcd} = 1.545 g cm^{−3}, final *R* = 0.0407, *wR* = 0.0996, GOF = 1.111 with *I* > 2.00σ(*I*). Crystal data for [Pd(en)₂][PdBr₂(en)](C₈H₁₇SO₃)₄·2H₂O at 93(2) K: *M*_r = 711.09, monoclinic, space group C2/c, *a* = 37.762(8) Å, *b* = 5.3018(9) Å, *c* = 15.290(4) Å, β = 97.060(11)°, *V* = 3037.9(11) Å³, *Z* = 4, ρ_{calcd} = 1.555 g cm^{−3}, final *R* = 0.0489, *wR* = 0.1048, GOF = 1.120 with *I* > 2.00σ(*I*). Crystal data for [Pd(en)₂][PdBr₂(en)](C₉H₁₉SO₃)₄·2H₂O at 93(2) K: *M*_r = 739.14, monoclinic, space group C2/c, *a* = 41.31(2) Å, *b* = 5.274(3) Å, *c* = 15.234(9) Å, β = 93.456(7)°, *V* = 3313(3) Å³, *Z* = 4, ρ_{calcd} = 1.482 g cm^{−3}, final *R* = 0.0455, *wR* = 0.0919, GOF = 1.143 with *I* > 2.00σ(*I*). Crystal data for [Pd(en)₂][PdBr₂(en)](C₁₀H₂₁SO₃)₄·2H₂O at 93(2) K: *M*_r = 767.19, monoclinic, space group C2/c, *a* = 42.75(3) Å, *b* = 5.292(4) Å, *c* = 15.311(11) Å, β = 99.086(9)°, *V* = 3420(4) Å³, *Z* = 4, ρ_{calcd} = 1.490 g cm^{−3}, final *R* = 0.0471, *wR* = 0.0909, GOF = 1.142 with *I* > 2.00σ(*I*). Crystallographic dates have been deposited with Cambridge Crystallographic Date Centre: Deposition number CCDC-291564, 291565, 291566, and 291567 for compound *n* = 7, 8, 9, and 10, respectively. Copies of the date can be obtained free of charge via <http://www.ccdc.cam.ac.uk/conts/retrieving.html> (or from the Cambridge Crystallographic Date Centre, 12, Union Road, Cambridge, CB2 1EZ, UK; Fax: +44 1223 336033; e-mail: deposit@ccdc.cam.ac.uk).

Polarized reflectivity spectra were obtained by using a specially designed spectrometer with a 25 cm grating monochromator and an optical microscope.

This work was partly supported by a Grant-in-Aid for Creative Scientific Research from the Ministry of Education, Culture, Sports, Science and Technology.

References

- a) J. S. Miller, *Extended Linear Chain Compounds*, New York and London, **1982**, Vols. I–III. b) A. R. Bishop, B. I. Swanson, *Los Alamos Sci.* **1993**, 21, 133. c) R. J. H. Clark, *Adv. Infrared Raman Spectrosc.* **1983**, 11, 95. d) G. C. Papavassiliou, A. D. J. Zdetsis, *J. Chem. Soc., Faraday Trans. 2* **1980**, 76, 104. e) H. Tanino, K. Kobayashi, *J. Phys. Soc. Jpn.* **1983**, 52, 1446. f) N. Kuroda, M. Sakai, Y. Nishina, M. Tanaka, S. Kurita, *Phys. Rev. Lett.* **1987**, 58, 2122. g) Y. Wada, K. Era, M. Yamashita, *Solid State Commun.* **1988**, 67, 953. h) R. Donohoe, S. A. Ekberg, C. D. Tait, B. I. Swanson, *Solid State Commun.* **1989**, 71, 49. i) Y. Iwasa, E. Funatsu, T. Hasegawa, T. Koda, M. Yamashita, *Appl. Phys. Lett.* **1991**, 59, 2219. j) R. J. Donohoe, L. A. Worl, C. A. Arrington, A. Bulou, B. I. Swanson, *Phys. Rev. B* **1992**, 45, 13185. k) H. Ooi, M. Yoshizawa, M. Yamashita, T. Kobayashi, *Chem. Phys. Lett.* **1993**, 210, 384. l) H. Okamoto, Y. Kaga, Y. Shimada, Y. Oka, Y. Iwasa, T. Mitani, M. Yamashita, *Phys. Rev. Lett.* **1998**, 80, 861.
- a) D. Baeriswyl, A. R. Bishop, *J. Phys. C: Solid State Phys.* **1988**, 21, 339. b) A. Mishima, K. Nasu, *Phys. Rev. B: Condens. Matter. Mater. Phys.* **1989**, 39, 5758.
- M. B. Robin, P. Day, *Adv. Inorg. Radiochem.* **1967**, 9, 247.
- H. Okamoto, K. Toriumi, K. Okaniwa, T. Mitani, M. Yamashita, *Mater. Sci. Eng., B* **1992**, 13, L9.
- Y. Wakabayashi, N. Wakabayashi, M. Yamashita, T. Manabe, N. Matsushita, *J. Phys. Soc. Jpn.* **1999**, 68, 3948.
- a) K. Toriumi, Y. Wada, T. Mitani, S. Bandow, M. Yamashita, Y. Fujii, *J. Am. Chem. Soc.* **1989**, 111, 2341. b) H. Okamoto, K. Toriumi, T. Mitani, M. Yamashita, *Phys. Rev. B* **1990**, 42, 10381. c) H. Okamoto, Y. Shimada, Y. Oka, A. Chainani, T. Takahashi, H. Kitagawa, T. Mitani, K. Toriumi, K. Inoue, T. Manabe, M. Yamashita, *Phys. Rev. B* **1996**, 54, 8438.
- H. Kishida, H. Matsuzaki, H. Okamoto, T. Manabe, M. Yamashita, Y. Taguchi, Y. Tokura, *Nature* **2000**, 405, 929.
- a) M. Yamashita, T. Ishii, H. Matsuzaka, T. Manabe, T. Kawashima, H. Okamoto, H. Kitagawa, T. Mitani, K. Marumoto, S. Kuroda, *Inorg. Chem.* **1999**, 38, 5124. b) K. Marumoto, S. Kuroda, T. Manabe, M. Yamashita, *Phys. Rev. B* **1999**, 60, 7699.
- S. Takaishi, H. Miyasaka, K. Sugiura, M. Yamashita, H. Matsuzaki, H. Kishida, H. Okamoto, H. Tanaka, K. Marumoto, H. Ito, S. Kuroda, T. Takami, *Angew. Chem., Int. Ed.* **2004**, 43, 3171.
- N. Matsumoto, M. Yamashita, S. Kida, *Bull. Chem. Soc. Jpn.* **1978**, 51, 2334.
- A. Taira, N. Matsushita, *Mol. Cryst. Liq. Cryst.* **2002**, 379, 297.
- M. Yamashita, K. Toriumi, T. Ito, *Acta. Crystallogr., Sect. C* **1985**, 41, 876.
- a) K. Prassides, P. Shatz, K. Wong, P. Day, *J. Phys. Chem.* **1986**, 90, 5588. b) K. Prassides, P. Shatz, *Chem. Phys. Lett.* **1991**, 178, 227.
- Y. Wada, T. Mitani, M. Yamashita, T. Koda, *J. Phys. Soc. Jpn.* **1985**, 54, 3143.